Applied Acoustics 202 (2023) 109108

Contents lists available at ScienceDirect

Applied Acoustics

journal homepage: www.elsevier.com/locate/apacoust

Estimation of the Rod Velocity in Wood using Multi-frequency Guided Wave Measurements

Adli Hasan Abu Bakar, Mathew Legg *, Daniel Konings, Fakhrul Alam

Department of Mechanical and Electrical Engineering, Massey University, Auckland, New Zealand

ARTICLE INFO

Article history:
Received 24 August 2022
Received in revised form 18 October 2022
Accepted 2 November 2022

Keywords:
Wood
Aluminium
ToF
Resonance
Guided waves
Dispersion curves

ABSTRACT

This study presents a new approach for measuring the acoustic "rod velocity" in wood using guided wave measurements. The approach fits the acoustic guided wave longitudinal L(0,1) wave mode dispersion curve, through experimental guided wave phase velocity measurements taken over a range of frequencies. The rod velocity is obtained by measuring the phase velocity of the fitted L(0,1) wave mode dispersion curve at zero frequency. This technique is used to obtain rod velocity measurements for cylindrical wood and aluminium samples. The same approach was also performed on resonance measurements at a wide range of harmonics. These rod velocities are then compared to acoustic velocities obtained using the traditional time of flight and resonance methods.
© 2022 The Authors. Published by Elsevier Ltd. This is an open access article under the CC BY license (http://creativecommons.org/licenses/by/4.0/).

1. Introduction

The ability to measure the properties of wood such as stiffness is important for the forestry industry. For example, segregation of logs according to stiffness before processing can lead to an increase in profitability and efficiency [1,2]. The static bending test is the gold standard technique for measuring the stiffness of timber [3]. However, ideally the stiffness of wood should be known before it is processed to ensure it is suitable for the desired product. Various Non-destructive Testing (NDT) techniques have therefore been developed to measure the stiffness of wood such as Near Infrared (NIR) spectroscopy [4], SilviScan [5], and acoustics [6].

Acoustics is the main technique used for measuring the stiffness of wood as it is inexpensive, simple to use and non-destructive. The stiffness of wood is related to the Modulus of Elasticity (MoE) in the longitudinal direction. The relationship between acoustic velocity c_o in the longitudinal direction and the modulus of elasticity E is commonly described using the classical 1D wave equation

$$c_o = \sqrt{\frac{E}{\rho}}, \tag{1}$$

where ρ is the density. This is often referred to as the rod velocity.

The Time-of-Flight (ToF) method is the common method used for measuring the acoustic velocity in standing trees. It can also be used with felled logs and timber samples [7]. Two probes are typically inserted into a sample and separated by a distance Δd. These are used to measure stress waves generated by either a hammer hit or an ultrasonic transducer which propagate along the sample. The acoustic velocity is then measured using

$$c_{tof} = \frac{\Delta d}{T}, \tag{2}$$

where T is the time taken for the signal to propagate between the two probes. This "time of flight" is predominantly measured using the amplitude threshold method. This uses a threshold to determine when the signal first goes above a threshold voltage at each transducer. The First Time of Arrival (FToA) technique only looks at the very start of the signal and ignores the rest of the signal. This technique will be referred to here as the traditional ToF method. This method has been shown to result in measurements of acoustic velocities that vary with the threshold value used, the hammer hit strength, and the noise level in the signal [8,9].

The acoustic resonance method is the main method used to measure the acoustic velocity for felled logs and timber samples, but cannot be used for standing trees. This technique predominantly uses stress waves generated by a hammer hit at one end of the log or timber specimen in the direction parallel to the grain. The stress waves are reflected from the ends of the sample multiple times resulting in standing waves. A device at one end of the

* Corresponding author.
E-mail addresses: A.Hasan@massey.ac.nz (A.H.A. Bakar), M.Legg@massey.ac.nz (M. Legg), D.Konings@massey.ac.nz (D. Konings), F.Alam@massey.ac.nz (F. Alam).

https://doi.org/10.1016/j.apacoust.2022.109108
0003-682X/© 2022 The Authors. Published by Elsevier Ltd.
This is an open access article under the CC BY license (http://creativecommons.org/licenses/by/4.0/).

sample records the signal and the spectrum is measured. The longitudinal resonance acoustic velocity can then be calculated using

$$c_{res} = \frac{2Lf_n}{n}, \quad (3)$$

where f_n is the n^{th} resonant frequency, n is an integer (1, 2, 3...) and L is the length of the specimen. This will be referred to here as the traditional resonance method. The second harmonic is commonly used for acoustic velocity determination in logs [10]. However, the fundamental frequency has also been used [6]. Note that flexural vibration techniques have also been used by researchers where a hammer hit is performed normal to the grain [11].

Studies have also shown that the acoustic velocity obtained using the ToF method has higher noise and is systematically higher than that of the resonance method [6,12–14]. This reported overestimation can be up to 36% and can vary with factors such as the diameter, age, and slenderness of the tree stem. This results in the ToF method having a systematic overestimation in stiffness measurements compared to those obtained using both resonance and static bending tests. There have been some suggestions made as to why this overestimation may be occurring [6,14]. For example, it is believed that the overestimation may be due to the ToF technique measuring bulk waves while the resonance technique measures the slower "rod waves". However, this topic still remains a key area where more fundamental research is needed.

Another area where questions have been raised by researchers is related to the harmonics used for obtaining the resonance acoustic velocity. Studies have reported that the measured resonance velocity varies depending on which harmonic frequencies are used. Andrews [12] reported measuring resonance frequencies that were not integer-multiple harmonics of each other. Chauhan and Walker [16] reported that the measured resonance velocities obtained using the first and second harmonic could differ by as much as 11%. Similarly, Hansen [16] reported differences in the velocities of up to 9% between the first five harmonics for pine and eucalyptus samples. Andrews [12] suggested that the tapered shape of the log could be the cause of the variation. However, the exact cause is still not known and more research is needed in this area.

Ultrasonic guided wave testing is a technique that is extensively used for structural health monitoring of metal structures such as oil and gas pipelines [17–20]. However, the use of acoustic/ultrasonic guided waves in wood is still in very early stages. Several lab-based studies have used measurements of the phase or group velocity of the guided wave modes to measure wood properties [21–25]. These studies were performed on rectangular cross-section timber samples which generate Lamb waves, which is different to the rod waves generated in cylindrical rods that are used in this study. Also, previous studies have not investigated the relationship between acoustic velocity measurements obtained using acoustic/ultrasonic guided waves and those obtained using the traditional ToF and resonance methods. Bakar et al. [26] showed that the ToF and resonance acoustic velocities in wooden and aluminium rods were roughly correlated with the longitudinal L(0,1) wave mode at low frequencies in the experimentally measured wavenumber-frequency dispersion curves plots. However, guided wave velocity measurements were not calculated from these wavenumber dispersion curves due to the low resolution of the 2D Fast Fourier Transform (FFT) method used [27].

This work presents a new approach that uses multi-frequency fitting of the guided wave fundamental longitudinal L(0,1) wave mode measurements to provide more accurate acoustic velocity measurements for wood property estimation. To the best of the author's knowledge, this is the first time this method has been used on resonance and guided wave measurements for wood. This work also compares acoustic velocity measurements obtained using the ToF, resonance and guided waves techniques for 16 mm diameter cylindrical aluminium and wood samples. We are not aware of any previous studies which have compared all three techniques for any type of material.

The remainder of the paper is organised as follows. Section 2 provides background theory. Section 3 describes the methodology and experimental procedure. Section 4 presents the experimental results. Lastly, Section 5 provides a conclusion and suggestions for future work.

2. Background theory

The classical 1D wave theory which is given by Eq. 1 is widely used due to its simplicity and gives good approximations at low frequencies. It ignores dispersion and suggests that the longitudinal wave mode propagates at a single velocity called the "rod velocity". An acoustic signal propagating through a rod-like sample should initially propagate as bulk waves. However, the signal may become a guided wave after travelling a sufficient distance along the sample if the diameter is small enough relative to the wavelength. These guided waves propagate as different types of vibrations called wave modes, which propagate at different velocities and are generally dispersive. Dispersion is caused by different frequency components in a wave mode propagating at different velocities, resulting in the signal spreading out as it propagates.

Dispersion of waves propagating in rod-like structures occurs due to the geometric and viscoelastic properties of the material [28]. There are three types of wave modes for a rod-like structure: longitudinal, flexural and torsional modes. Dispersion curves describe the propagation speed in a medium and can be represented by plotting the phase velocity, group velocity or wavenumber as a function of frequency [29]. Dispersion curves can be obtained by solving the Pochammher-Chree (PC) equation [30–32] which is considered the exact theory. The exact solution to the PC equation describes the three-dimensional wave propagation of the longitudinal, torsional and flexural wave modes in cylindrical rods of infinite length. The solution is complex and is restricted to bars of circular cross-section and infinite length [33].

Since the longitudinal wave mode is widely used for engineering applications [34], several approximate theories have been developed to describe the wave propagation of the L(0,1) longitudinal wave mode. Examples of these approximate theories include the Rayleigh-Love [35], Rayleigh-Bishop [36] and Mindlin-Hermann [37] theories. These theories represent dispersive systems where the phase velocity of the longitudinal L(0,1) wave mode is a function of frequency. The exact solution to the PC equation is normally used as a reference to determine the accuracy of these approximate theories.

As an alternative to the exact theory, analytical methods have been developed to model the wave propagation in a material. Among them, the Semi-Analytical Finite Element (SAFE) method is widely used and is accurate [38]. GUIGUW [39] is an example of a free software that uses the SAFE method to obtain dispersion curves. Fig. 1 shows the theoretical dispersion curves obtained using GUIGUW for a 16 mm diameter aluminium rod with an assumed density of 2,710 kg/m^3, Poisson's ratio of 0.33 and Young's Modulus of 68.9 GPa. These dispersion curves show that for the frequency range shown here, only the fundamental longitudinal L(0,1), torsional T(0,1) and flexural wave F(1,1) modes are present. (Note that higher order wave modes may start propagating if either the frequency or diameter is increased). The fastest wave mode is the longitudinal wave mode. At low frequencies, the longitudinal wave mode propagates at the rod velocity given by Eq. 1. The rod velocity c_o in cylindrical rods corresponds to the velocity of the fundamental longitudinal wave mode L(0,1) at zero frequency [32,41–42]. As the frequency increases, the mea-

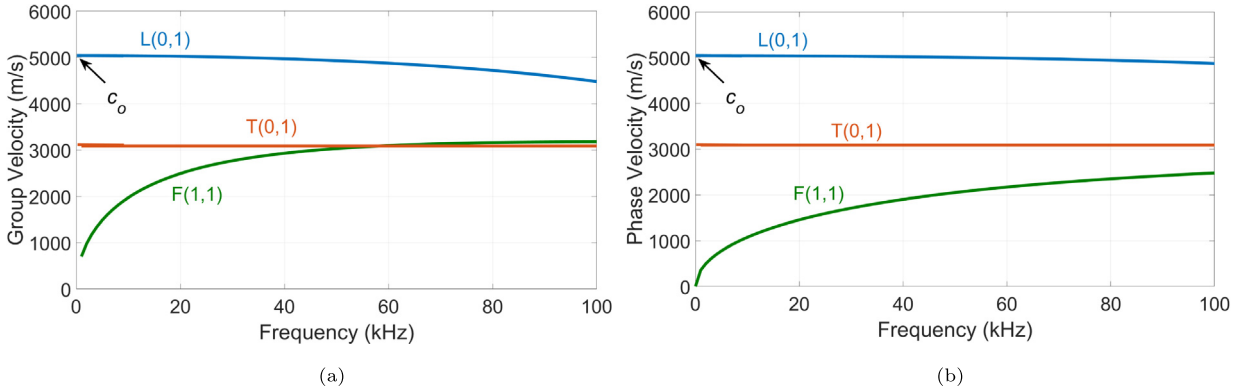

Fig. 1. Theoretical dispersion curves for a 16 mm diameter aluminium rod showing the (a) group and (b) phase velocities. Also shown is the rod velocity c_o, which is the longitudinal velocity as the frequency goes to zero.

sured acoustic velocity will be lower than the rod velocity due to dispersion.

If the L(0,1) wave mode was able to be excited at very low frequencies, its phase velocity should ideally correspond to the rod velocity allowing one to calculate the MoE by rearranging Eq. 1 to give

$$E = \rho c_o^2. \tag{4}$$

However, the guided wave phase velocity measurements for higher frequencies should produce a phase velocity that is lower than the rod velocity c_o due to dispersion. This could lead to an underestimation in the calculated MoE. This underestimation should depend on the radius and Poisson's ratio for an isotropic cylindrical sample. However, it should be noted that the wave propagation is more complex for wood, which is orthotropic and hence has more than one Poisson's ratio [14].

Acoustic resonance has been used, mainly in early works, to measure dispersion curves for metal rods [43–47]. Eq. 3 is used over a wide range of resonant frequencies to obtain experimental measurements of the L(0,1) phase velocity dispersion curve. Brizard [47] reported that at the lower frequencies, the resonance technique is prone to larger errors due to frequency resolution issues. Brizard used fitting of multi-frequency resonance measurements to obtain rod velocity and Poisson's ratio measurements for a steel bar in Split Hopkinson Bar (SHB) testing. This technique has not been used before for wood. Additionally, we have not found any previous papers that have used multi-frequency guided wave measurements to obtain the rod velocity for wood. Shin [48,49] also obtained rod velocity and Poisson's ratio measurements for steel rods but this was related to a dispersion correction technique in SHB measurements.

In this work, we used a somewhat similar approach to the one presented by Brizard [47]. The resonance velocities for a wood sample were calculated using Eq. 3 for a range of harmonic frequencies and a curve was fitted across the measurements to obtain the rod velocity c_o. Additionally, this work extends the work presented by Brizard by obtaining the rod velocity of wood using guided wave phase velocity measurements where narrow bandwidth signals are used to excite the fundamental L(0,1) wave mode. These rod velocities are compared with the acoustic velocities obtained using traditional resonance and ToF methods.

3. Methodology

Kiln-dried radiata pine rods with diameters of 16 and 40 mm that were 2460 mm in length were obtained. The samples were selected such that they were defect-free and did not have any observable knots, cracks or damage. Additionally, a T6 temper 6061 aluminium rod with a diameter of 16 mm and a length of 2510 mm was also used to provide a comparison.

Fig. 1 shows the theoretical dispersion curves for a 16 mm diameter aluminium rod. The figure shows that at frequencies below 100 kHz, no higher order wave modes are present and only the fundamental longitudinal L(0,1), flexural F(1,1) and torsional T(0,1) wave modes exist. Both the longitudinal and flexural wave modes are observed to be dispersive whereas the torsional wave mode is not. Using the above parameters, the calculated bulk wave speed for aluminium is approximately 6,175 m/s [14], which is significantly higher than the rod velocity.

Theoretical dispersion curves for wood are not provided here since the mechanical properties of the sample were not known. Refer to our previous article [26] for examples of wavenumber dispersion curve measurements for both the aluminium and wood samples where the same three wave modes were shown to be generated in both the aluminium and wood samples.

3.1. Resonance measurements

For resonance measurements, a hammer hit was performed parallel to the grain at one exposed end of the sample to generate longitudinal vibrations. At the opposite end of the sample, a GRAS 46BF-1 microphone [50] that has a bandwidth of 4 Hz - 100 kHz was used to measure the received signal. The microphone was connected to a GRAS 26A-1 pre-amp and powered by a GRAS 12AK power module. The received signal from the microphone was sampled at 2 MHz using the Analog to Digital Converter (ADC) channel from a Data Translation DT9832 data acquisition module. This setup can be seen in Fig. 2.

An FFT was performed on the sampled data and the resonant frequencies were identified. Resonance acoustic velocities were calculated from each resonance frequency peak over a wide frequency range using Eq. 3. As discussed in the previous section, this should provide an experimental measurement of the longitudinal L(0,1) phase velocity dispersion curve for the aluminium and wood samples.

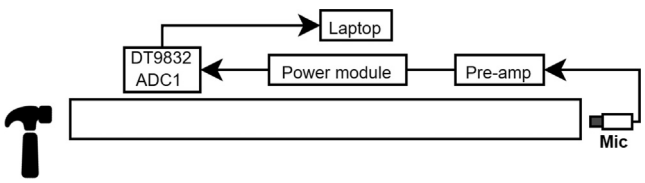

Fig. 2. Experimental setup resonance measurements.

3.2. ToF measurements

For wood related studies, probes are traditionally inserted into a wood sample to penetrate the bark. This allows good coupling between acoustic signals and the wood sample. However, in this work, shear PZT transducers produced by The Welding Institute (TWI), UK were directly coupled onto the sample by clamping them using springs as shown in Fig. 3. The transducers are broadband and have a relatively flat frequency response for the frequency range used in this study [51].

Two shear transducers were used to receive vibrations and were positioned as shown in Fig. 4. The contact face of the transducers were oriented parallel to the wood grain to enhance the reception of longitudinal vibrations. A hammer impact was performed parallel to the grain at one end of the sample. The recording of the received signal was initiated by a keyboard button press just before the hammer hit was performed. Transducers RX1 and RX2 were directly connected to the ADC channels of the DT9832 module and sampled at 2 MHz. The received signal was saved to file for further post-processing. Amplitude thresholding was used to determine the First Time of Arrival (FToA) of the received signals. The ToF velocity was then calculated using Eq. 2.

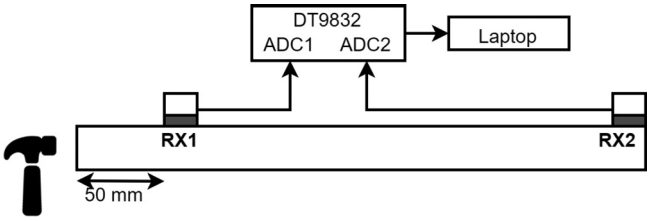

Fig. 4. Experimental setup ToF measurements.

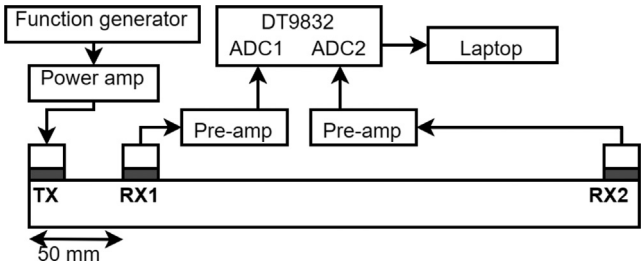

Fig. 5. Experimental setup for guided wave measurements.

3.3. Guided wave measurements

For guided wave measurements, three shear transducers were used and positioned as seen in Fig. 5. The contact faces of the transducers were oriented parallel to the grain to enhance the excitation and reception of longitudinal vibrations. The transducers were directly clamped onto the sample using springs. The excitation signal applied to the transmit transducer (TX) was created in MATLAB. For transmission, five cycles of a Hanning windowed sine wave with central frequencies f_o ranging from 15 to 50 kHz were used and outputted using an Agilent 33220A Function Generator. A custom-made linear power amplifier was then used to amplify the outputted signal to amplitudes of up to 400 Vpp. The receivers were connected to pre-amps and the received signal at RX1 and RX2 were sampled at 2 MHz using the ADC channels from the DT9832 module and saved to file.

Phase velocity measurements were performed using the guided wave measurements to obtain the phase velocity dispersion curve for the L(0,1) wave mode. The phase velocities were obtained using a frequency-domain shifting technique. For each transmission, the received signal at RX1 was converted into the frequency domain using a FFT. Eq. 5 below was then used to simulate the propagation of the frequency-domain received signal $G(\omega)$ by a distance d using an initial phase velocity $v_{ph}(\omega)$ and attenuation $\alpha(\omega)$.

$$Y(\omega) = G(\omega)e^{-j\left(\frac{\omega}{v_{ph}(\omega)}\right)d-\alpha(\omega)d}. \quad (5)$$

The distance between RX1 and RX2 receivers was used as the distance d. The propagated signal $Y(\omega)$ was then converted back into the time-domain using an Inverse Fast Fourier Transform (IFFT). The Root Mean Squared Error (RMSE) between the propagated time-domain signal RX1 and RX2 was calculated. The phase velocity v_{ph} was adjusted by 1 m/s until a minimum RMSE was obtained. This process was repeated for a range of central transmit frequencies f_o.

3.4. Rod velocity estimation

Eq. 4 allows us to calculate the MoE from the rod velocity c_o, which is the phase velocity of the L(0,1) wave mode at low frequencies. However, as discussed in Section 2, at higher frequencies, the phase velocity of this wave mode will be lower than the rod

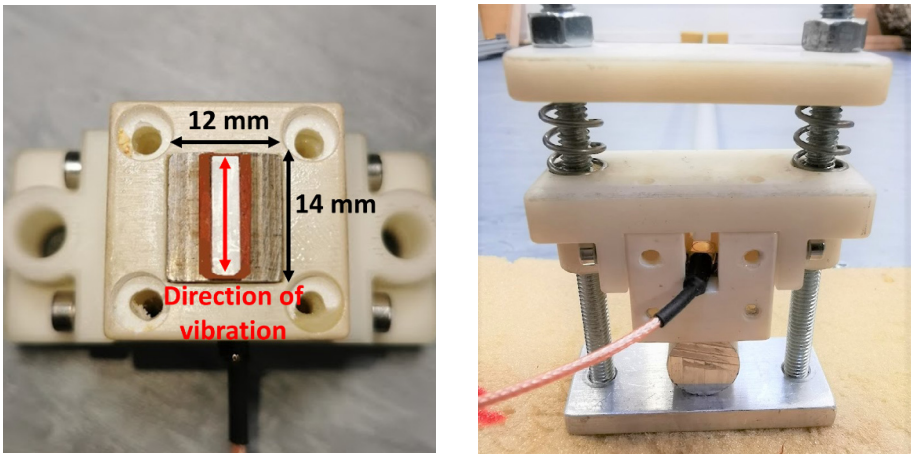

(a) (b)

Fig. 3. Photo (a) shows one of the transducers used in this experiment. Photo (b) shows the transducer being pushed against an aluminium rod sample using springs.

velocity leading to an underestimation in the estimated MoE using this equation. A fitting technique was used that estimates the rod velocity at zero frequency using experimental measurements of the phase velocity of the L(0,1) wave mode at a range of frequencies. This technique is used for both the resonance and guided wave measurements. In this paper, the terms resonance rod velocity and guided wave rod velocity corresponds to the phase velocity at zero frequency that is obtained by fitting a dispersion curve through the experimental resonance or guided wave measurements. A curve of best fit was obtained using the following equation

$$c_l = c_o\sqrt{\frac{1+\alpha_1\alpha_2 k^2}{1+\alpha_1 k^2}}, \tag{6}$$

where c_o is the rod velocity, α_1 and α_2 are constants and k is the wavenumber. The optimum values for variables c_o, α_1 and α_2 were obtained using a non-linear least squares fitting technique performed in MATLAB. The equation is based on the correction for the Rayleigh-Bishop theory [52]. The equation was chosen as it is simple to use and gives good approximations at "low" to "medium" wavenumbers. More accurate approximations at "large" wavenumbers can be obtained using higher-order rod approximations such as the Mindlin-McNevin theory [53] or the one proposed by Anderson [54]. These approximations are more accurate over larger range of wavenumbers but are much more complex. Eq. 6 should be sufficient to characterize the dispersion curve of the L(0,1) wave mode for the frequency range of interest in this current work.

4. Results

Fig. 6 shows a comparison of the acoustic velocities obtained using the different methods at varying frequencies for the 16 mm diameter aluminium and wood samples. The theoretical L(0,1) dispersion curve for the aluminium sample obtained using GUIGUW was overlaid onto the figure. However, the same could not be done for the wood sample as the mechanical properties are not known. Note that the experimental frequency range for the wood sample is lower than the aluminium sample because wood suffers from a stronger degree of attenuation at higher frequencies. The hammer hit ToF measurements are not frequency dependent and hence these measurements have been represented in these plots as a grey shaded region, which shows the variation of the ToF acoustic velocities.

Table 1 shows the average acoustic velocity and uncertainties for each method. The traditional ToF velocities are obtained from the average of 100 measurements per sample using a threshold value of 0.05 V. Traditionally, the resonance acoustic velocity for wood is obtained using either the fundamental or second harmonic. In this work, the average between the fundamental and second harmonic was taken as the average traditional resonance velocity.

For aluminium, the maximum error between the measured phase velocities for guided wave and resonance measurements compared with those obtained from the theoretical L(0,1) wave mode, as shown in Fig. 6, is approximately less than 0.8%. This shows that the L(0,1) wave mode is being excited and measured in this study. The same is expected for the wood sample. A discussion of the results for each method is presented in the subsections below.

4.1. Traditional time of flight

Fig. 7 shows an example of the received signal obtained using the ToF method for both the 16 mm diameter aluminium and wood samples. An amplitude threshold of 0.05 V was used as it was approximately 3 times the standard deviation of the noise and did not result in false positives. Note that the difference in arrival times is because the recording of the ToF received signals was initiated manually through a button press.

The ToF measurements used in this work are obtained using the amplitude thresholding method, which measures the FToA of the signal. It will therefore obtain velocity measurements using the frequency component of the signal with the fastest phase velocity. If we assume that only the longitudinal L(0,1) wave mode is propagating, this speed should ideally correspond to the rod velocity at zero frequency. However, the traditional ToF velocities are observed to be higher than the traditional resonance velocities and the fitted resonance and guided wave rod velocities. It does not appear that this is due to the ToF technique measuring the bulk wave speed in this case, as we know that the bulk wave speed for aluminium (6175 m/s) is much higher than the results we obtained. Instead, this is most likely due to the first part of the

Table 1
Acoustic velocity measurements for 16 mm diameter aluminium and wood samples using different methods.

Method	Acoustic velocity (m/s)	
	Aluminium	Wood
Average traditional ToF	5106 ± 12	4574 ± 46
Average traditional resonance	5031 ± 13	4392 ± 24
Fitted resonance rod velocity	5029	4463
Fitted guided wave rod velocity	5062	4526

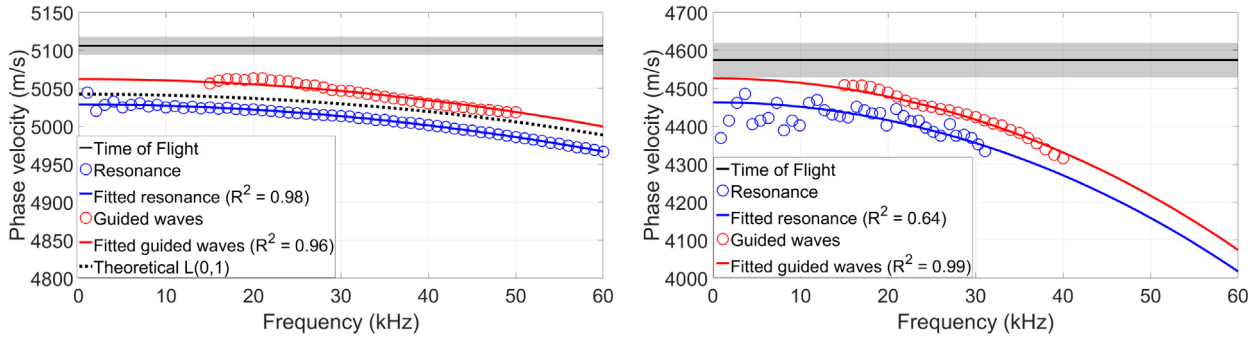

(a) (b)

Fig. 6. Plots of acoustic velocity measured using resonance, ToF and guided waves plotted as a function of frequency for the 16 mm diameter (a) aluminum and (b) wooden samples. Overlaid are the fitted dispersion curves which are used to estimate the rod velocity. For the aluminium sample, the theoretical L(0,1) dispersion curve has also been overlaid.

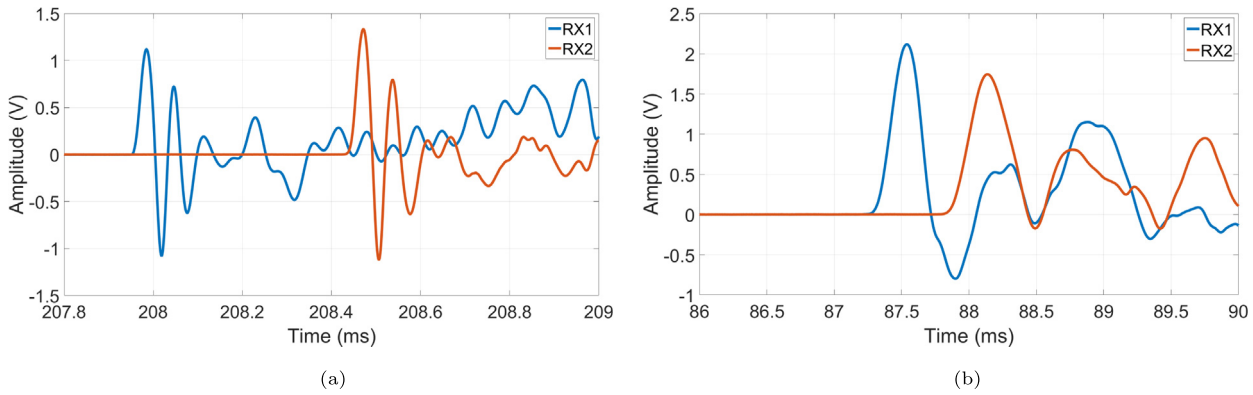

Fig. 7. Plots of the received signal for ToF experiment for (a) aluminium and (b) wood samples.

received signal being distorted due to dispersion effects [55,56]. This could potentially affect ToF measurements obtained using the amplitude threshold method.

4.2. Resonance

Fig. 8 shows the measured resonance frequencies for the 16 mm diameter aluminium and wood samples. The wood sample has high attenuation, which results in a limited frequency range compared to the aluminium sample.

The results presented in Fig. 6 show that the resonance velocity decreases with increasing frequency and follows a curve. The figure also shows that there is some variation in the measured resonance velocities, which decreases at higher frequencies. One factor that could be causing this is the resolution of the measured resonance velocity. The frequency resolution (resolution of the FFT) is defined as $\Delta f = f_s/N$ where f_s is the sampling frequency and N is the number of samples. Substituting this into Eq. 3, the resolution (quantisation) of the measured resonance velocity can be calculated as

$$\Delta c = \frac{2Lf_s}{nN}. \tag{7}$$

The resolution of the measured resonance velocity is therefore inversely proportional to the harmonic integer n. As the harmonic integer increases, the resolution of the resonance velocity decreases asymptotically. This explains why the variation in resonance measurements decreases with an increase in frequency. This can be mitigated by using a longer recording time of the received signal. As the recording time increases, the number of samples N also increases hence the resolution of the measured resonance velocity Δc decreases. However, increasing the recording time could cause high frequency components to be reduced due to attenuation. It can also be seen that there is more variation in the measured resonance velocities for wood compared to those obtained for the aluminium sample. This may be because of higher attenuation rates or because wood is orthotropic and inhomogeneous.

4.3. Guided waves

Fig. 6 shows that the longitudinal L(0,1) guided wave velocity measurements for 16 mm diameter wood and aluminium samples decrease with an increase in frequency and roughly follow the traditional resonance measurements. However, the guided wave phase velocity values are systematically slightly higher than those for resonance at a given frequency. The similarity in the curve produced between the guided wave measurements for the 16 mm diameter aluminium and wood gives us the confidence that the measurements performed on wood are reliable. The phase velocities for frequencies below 15 kHz could not be reliably measured as the received signals were highly distorted due to the long wavelengths and reflections from the ends of the samples. Using samples with a longer length could allow lower frequencies to be used as the signal would have time to finish transmission before reflections occur.

The phase velocity measurements obtained using the guided wave method were very repeatable. The measured guided wave phase velocities were found to be independent of the amplitude of the transmit signal. This is because the method matches the peaks of the entire waveform. No difference in the measured velocity was observed for each sample when velocity measurements were repeated across multiple recordings for a given transmission frequency. It therefore provides more consistent results than the

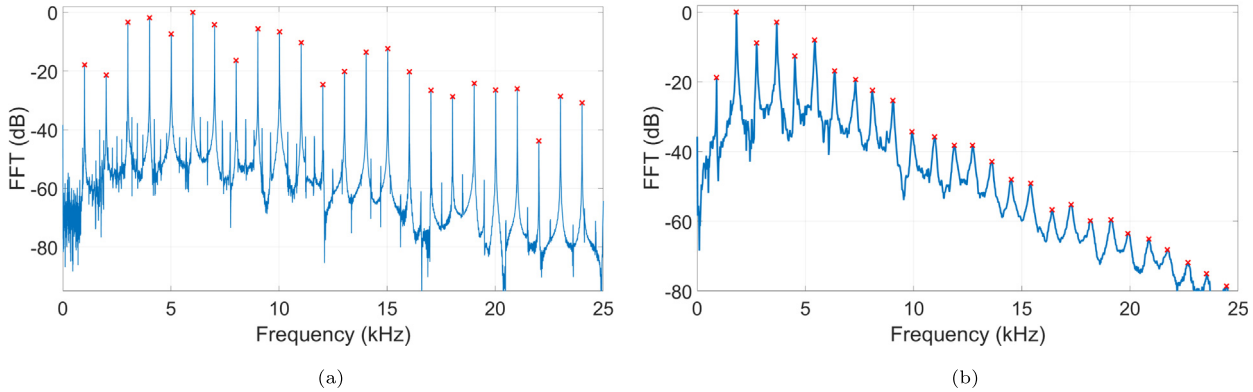

Fig. 8. Plot showing the resonance frequencies (marked red) for the 16 mm (a) aluminium and (b) wood samples.

traditional ToF method but produces acoustic velocities that vary with frequency.

4.4. Resonance and guided wave rod velocity

As discussed above, both the resonance and guided wave phase velocity measurements follow the L(0,1) wave mode dispersion curve and hence vary with frequency. A curve was fitted through the experimental resonance measurements using Eq. 6 to obtain the rod velocity. A resonance rod velocity of 5029 m/s and 4463 m/s were obtained for the aluminium and wood samples respectively. The difference between the traditional resonance velocity and the resonance rod velocity is approximately 0.03% and 1.61% for the aluminium and wood samples respectively.

In order to quantify the goodness-of-fit of the fitted dispersion curve, the coefficient of determination or R^2 value is used. The R^2 value indicates the proportion of variance in the dependent variable that can be explained by the independent variable. In this study, the R^2 value measures the amount of variation in the experimental data that can be explained by the fitted regression model. The R^2 values (0.98 for aluminium and 0.64 for wood) show that the fitted dispersion curves match well with the experimental traditional resonance measurements. The R^2 value for the wood sample is smaller than the aluminium sample as there is more variation in resonance measurements for the wood sample. This may be due to the highly attenuative nature of wood or because wood is orthotropic and inhomogenous.

Dispersion curves were also fitted through the experimental guided wave phase velocity measurements for both aluminium and wood samples. For the aluminium sample, at the frequency range of interest, the fitted dispersion curves are observed to be close to the theoretical L(0,1) dispersion curve, as seen in Fig. 6. The maximum difference between the fitted resonance and guided wave dispersion curves relative to the theoretical L(0,1) dispersion curve for the aluminium sample are 0.4% and 0.3% respectively. The theoretical dispersion curve for the wood sample could not be obtained as the mechanical properties are not known. Guided wave rod velocities of 5062 m/s and 4526 m/s were obtained for the aluminium and wood samples respectively. The measured guided wave rod velocities are observed to be lower than the acoustic velocities obtained using the traditional ToF method but are slightly higher compared to the traditional resonance method. High R^2 values (0.96 for aluminium and 0.99 for wood) were obtained from the fitted dispersion curves using the guided wave phase velocity measurements. This shows that Eq. 6 provides a good approximation of the L(0,1) phase velocity dispersion curve for the samples used in this study in the frequency range of interest.

4.5. Results on larger diameter wood sample

Resonance, ToF and guided wave measurements were also performed on a 40 mm diameter wood sample. Fig. 9 shows a comparison of acoustic velocities obtained using these methods at varying frequencies for the 40 mm diameter wood sample. ToF acoustic velocities are observed to be significantly higher compared to the resonance and guided wave velocities. The frequency range where measurements were able to be reliably obtained was lower for both resonance and guided wave measurements compared to the 16 mm wood sample. There appears to be higher attenuation rates at higher frequencies for this sample relative to the 16 mm diameter wood sample. The resonance and guided wave phase velocity measurements decrease with an increase in frequency and follow a curve that is similar to the 16 mm diameter wood sample. Dispersion curves are fitted through the measurements using the method described in Section 3.4 and a high R^2 value (0.93) is obtained for the fitted dispersion curve for guided wave phase velocity measurements. However, a low R^2 value (0.27) is obtained for the resonance measurements which may be due to the measurement variations.

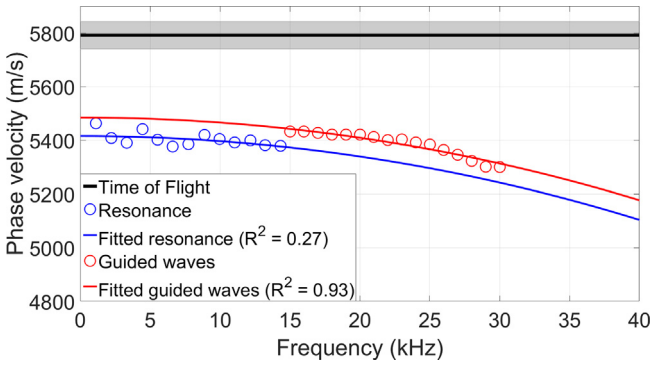

Fig. 9. Plot of acoustic velocity using ToF, resonance and guided wave plotted as a function of frequency for a 40 mm diameter wood sample. Overlaid are the fitted dispersion curves for the resonance and guided wave measurements.

Table 2
Average acoustic velocity obtained using different methods for a 40 mm diameter wood sample.

Method	Acoustic velocity (m/s)
Average traditional ToF	5792 ± 51
Average traditional resonance	5435 ± 37
Fitted resonance rod velocity	5416
Fitted guided wave rod velocity	5485

Table 2 shows a comparison of acoustic velocities obtained using different methods for the 40 mm diameter wood sample. The traditional ToF acoustic velocity is approximately 6.5% higher compared to the traditional resonance method. This ToF overestimation is significantly higher compared to the 16 mm diameter wood sample. The fitted guided wave rod velocity is closer to the traditional resonance velocity compared to the traditional ToF velocity. The results show that the fitting technique and guided wave phase velocity measurements can be used as an alternative to the traditional ToF method to obtain more accurate acoustic velocity measurements for wood.

5. Conclusion

The traditional acoustic resonance technique is commonly used for wood stiffness measurements as it is accurate and easy to use. However, it cannot be used on standing trees. In contrast, the traditional ToF method works on both standing trees and cut logs but literature has reported an overestimation using this measurement technique. This study investigated a new technique for obtaining the rod velocity of wooden samples using ultrasonic guided waves which can potentially be used for both standing trees and cut timber/logs.

The acoustic/ultrasonic guided wave phase velocity of the L(0,1) wave mode theoretically starts at the rod velocity at zero frequency and then decreases as the frequency increases. Therefore, to measure the rod velocity, the proposed technique performs measurements of the L(0,1) phase velocity at a range of frequencies and fits a curve through them to obtain an estimate of the phase velocity at zero frequency. This will correspond to the rod velocity of the sample. The same rod velocity fitting technique is also used

with resonance velocity measurements made using a range of resonance harmonics.

To test the proposed method, resonance, ToF and guided wave measurements were performed on cylindrical wooden rods with diameters of 16 and 40 mm and length of 2460 mm each. These measurements were repeated on a 16 mm diameter aluminium rod with a similar length for comparison. The guided wave longitudinal L(0,1) phase velocity measurements in the rod samples decrease with an increase in frequency. The fitted phase velocity dispersion curves matched well with the experimental phase velocity measurements for both aluminium and wood samples. The R^2 values of the fits were 0.99 and 0.93 for the wood samples and 0.96 for the aluminium sample. The fitted rod velocities matched well with the traditional resonance velocities. In contrast, the measured ToF velocities were higher compared to both the guided wave rod velocities and traditional resonance velocities, as shown in Table 3.

This same fitting technique was also used for the phase velocity measurements obtained using the multi-frequency resonance method. These measurements decreased with increased frequency and follow the phase velocity dispersion curve of the L(0,1) wave mode. The fitting technique was used to obtain the rod velocity in a similar manner to the guided wave measurements. The R^2 values of the fitting were lower than for the guided wave measurements (0.64 and 0.27 for the wood samples). This is related to the larger variance in the resonance measurements at lower frequencies, which appears to be related to the resolution of the FFT. Since the fitting technique uses higher frequency harmonics, this technique can be used to provide more accurate results compared to the traditional resonance technique, which only uses a single lower frequency resonance peak where the variances are larger. However, more work is needed to see if the higher frequency harmonics can be measured with samples that have a larger diameter and higher moisture content which may have higher attenuation rates.

Ultrasonic guided waves have previously been used on logs with large diameters [57]. Therefore, the guided wave technique presented in this study has the potential to be used as an alternative to the traditional ToF method to obtain acoustic velocity measurements for logs, standing trees and seedlings. Initial results from this study show that the guided wave fitting technique was more accurate compared to the traditional ToF method. This can result in more efficient segregation and sorting of logs before harvesting which could improve the sustainability and profitability of the forestry industry. This work shows that guided wave techniques can be used to obtain improved measurements of wood properties. Additionally, there is potential for the fitted resonance technique to provide more accurate rod velocity measurements for timber and log samples compared to the traditional resonance technique, which is considered to be the gold standard in acoustic non-destructive stiffness measurements for wood.

Future works should investigate the use of more accurate approximations of the longitudinal L(0,1) wave mode, as these might provide more accurate rod velocity measurements. Stiffness measurements obtained using the presented approach should also ideally be compared with those obtained using static bending tests. Also, measurements should be performed on larger diameter samples such as logs. This will allow the effect of higher order wave modes and potentially the presence of bulk waves to be evaluated.

Table 3
Difference in measured acoustic velocities obtained using the traditional ToF and the rod velocities obtained using the guided wave method relative to the traditional resonance velocity for wood.

Wood sample	Difference relative to resonance	
	Traditional ToF	Rod velocity
16 mm diameter	4.1%	3.0%
40 mm diameter	6.5%	0.9%

Declaration of Competing Interest

The authors declare that they have no known competing financial interests or personal relationships that could have appeared to influence the work reported in this paper.

References

[1] Achim A, Paradis N, Carter P, Hernández RE. Using acoustic sensors to improve the efficiency of the forest value chain in Canada: A case study with laminated veneer lumber. Sensors 2011;11(6):5716–28.
[2] Wang X, Carter P, Ross RJ, Brashaw BK. Acoustic assessment of wood quality of raw forest materials: a path to increased profitability. Forest Products J 2007;57(5):6–14.
[3] Hai PH, Hannrup B, Harwood C, Jansson G, Van Ban D. Wood stiffness and strength as selection traits for sawn timber in *Acacia auriculiformis*. Can J For Res 2010;40(2):322–9.
[4] Schimleck L, Matos J, Trianoski R, Prata J. Comparison of methods for estimating mechanical properties of wood by NIR spectroscopy. J Spectroscopy 2018.
[5] Ma T, Inagaki T, Tsuchikawa S. Non-destructive evaluation of wood stiffness and fiber coarseness, derived from SilviScan data, via near infrared hyperspectral imaging. J Near Infrared Spectrosc 2018;26(6):398–405.
[6] Wang X. Acoustic measurements on trees and logs: A review and analysis. Wood Sci Technol 2013;47(5):965–75.
[7] Wang X, Ross RJ, Carter P. Acoustic evaluation of wood quality in standing trees. Part I. Acoustic wave behavior. Wood Fiber Sci 2007;39(1):28–38.
[8] Rescalvo FJ, Ripoll MA, Suarez E, Gallego A. Effect of location, clone, and measurement season on the propagation velocity of poplar trees using the Akaike information criterion for arrival time determination. Materials 2019;12(3):356.
[9] Espinosa L, Bacca J, Prieto F, Lasaygues P, Brancheriau L. Accuracy on the time-of-flight estimation for ultrasonic waves applied to non-destructive evaluation of standing trees: a comparative experimental study. Acta Acustica united Acustica 2018;104(3):429–39.
[10] Harris P, Andrews M, Tools and acoustic techniques for measuring wood stiffness, in: Proceedings of the 3rd Wood Quality Symposium: Emerging Technologies For Evaluating Wood Quality for Processing, Forest Industry Engineering Association, Rotorua, New Zealand, 1999.
[11] Hassan KT, Horáček P, Tippner J. Evaluation of stiffness and strength of Scots pine wood using resonance frequency and ultrasonic techniques. BioResources 2013;8(2):1634–45.
[12] Andrews M, Where are we with sonics, in: Workshop 2000. Capturing the Benefits of Forestry Research: Putting Ideas to Work, Wood Technology Research Centre. University of Canterbury New Zealand, 2000, pp. 57–61.
[13] Ross RJ, Brashaw BK, Punches J, Erickson JR, Forsman JW, Pellerin RF, Wang X. Diameter effect on stress-wave evaluation of modulus of elasticity of logs. Wood Fiber Sci 2004;36(3):368–77.
[14] Legg M, Bradley S. Measurement of stiffness of standing trees and felled logs using acoustics: A review. J Acoust Society Am 2016;139(2):588–604.
[15] Chauhan S, Walker J. Variations in acoustic velocity and density with age, and their interrelationships in radiata pine. For Ecol Manage 2006;229(1):388–94.
[16] Hansen HJ. Acoustic studies on wood. University of Canterbury. School of Forestry; 2006. Ph.D. thesis.
[17] Olisa SC, Khan MA, Starr A. Review of current guided wave ultrasonic testing (GWUT) limitations and future directions. Sensors 2021;21(3):811.
[18] Ling EH, Abdul Rahim RH. A review on ultrasonic guided wave technology. Australian J Mech Eng 2020;18(1):32–44.
[19] Wang Z, Liu J, Wang K, Fang C, Wang L, Wu Z. Nondestructive measurements of elastic constants of thin rods based on guided waves. Mech Syst Signal Process 2022;170:108842.
[20] Pabisek E, Waszczyszyn Z. Identification of thin elastic isotropic plate parameters applying guided wave measurement and artificial neural networks. Mech Systems Signal Process 2015;64:403–12.
[21] Dahmen S, Ketata H, Ghozlen MHB, Hosten B. Elastic constants measurement of anisotropic Olivier wood plates using air-coupled transducers generated Lamb wave and ultrasonic bulk wave. Ultrasonics 2010;50(4–5):502–7.
[22] Fathi H, Kazemirad S, Nasir V. A nondestructive guided wave propagation method for the characterization of moisture-dependent viscoelastic properties of wood materials. Mater Struct 2020;53(6):1–14.
[23] Fathi H, Kazemirad S, Nasir V. Lamb wave propagation method for nondestructive characterization of the elastic properties of wood. Appl Acoust 2021;171:107565.
[24] Fathi H, Kazemirad S, Nasir V. Mechanical degradation of wood under ultraviolet radiation characterized by Lamb wave propagation. Structural Control Health Monitoring 2021;28(6):e2731.

[25] Fathi H, Nasir V, Kazemirad S. Prediction of the mechanical properties of wood using guided wave propagation and machine learning. Constr Build Mater 2020;262:120848.
[26] Bakar AHA, Legg M, Konings D, Alam F. Ultrasonic guided wave measurement in a wooden rod using shear transducer arrays. Ultrasonics 2022;119:106583.
[27] Alleyne D, Cawley P. A two-dimensional Fourier transform method for the measurement of propagating multimode signals. J Acoust Society Am 1991;89 (3):1159–68.
[28] Othman R, Gary G, Blanc R, Bussac M, Collet P. Dispersion identification using the Fourier analysis of resonances in elastic and viscoelastic rods. In: Acoustics, Mechanics, and the Related Topics of Mathematical Analysis. World Scientific; 2002. p. 229–35.
[29] Rose JL. Ultrasonic guided waves in solid media. Cambridge University Press; 2014.
[30] Chree C. The equations of an isotropic elastic solid in polar and cylindrical co-ordinates their solution and application. Trans Cambridge Philosophical Society 1889;14:250.
[31] Pochhammer L. Ueber die fortpflanzungsgeschwindigkeiten kleiner schwingungen in einem unbegrenzten isotropen kreiscylinder. Berlin/New York Berlin, New York: Walter de Gruyter; 1876.
[32] Davies R. A critical study of the Hopkinson pressure bar. Philos Trans R Soc London. Series A, Math Phys Sci 1948;240(821):375–457.
[33] Shatalov M, Marais J, Fedotov I, Tenkam MD, Schmidt M. Longitudinal vibration of isotropic solid rods: from classical to modern theories. Adv Computer Sci Eng 1877;2011:408–9.
[34] Xie L, Bian C, Wang J. Correction factors of the approximate theories for axisymmetric modes of longitudinal waves in circular rods. Acta Mech Solida Sin 2022:1–10.
[35] Love AEH. A treatise on the mathematical theory of elasticity. Cambridge University Press; 2013.
[36] Bishop R. Longitudinal waves in beams. Aeronaut Quarterly 1952;3(4):280–93.
[37] Mindlin R, A one-dimensional theory of compressional waves in an elastic rod, in: Proceedings of the First US National Congress of Applied Mechanics, 1951, pp. 187–191.
[38] Bartoli I, Marzani A, Di Scalea FL, Viola E. Modeling wave propagation in damped waveguides of arbitrary cross-section. J Sound Vib 2006;295(3–5):685–707.
[39] Bocchini P, Marzani A, Viola E. Graphical user interface for guided acoustic waves. J Computing Civil Eng 2011;25(3):202–10.
[40] Tefft WE, Spinner S. Cross-sectional correction for computing Young's modulus from longitudinal resonance vibrations of square and cylindrical rods. J Res National Bureau Standards A 1962;66:193–7.
[41] Zemanek Jr J, Rudnick I. Attenuation and dispersion of elastic waves in a cylindrical bar. J Acoust Society Am 1961;33(10):1283–8.
[42] Rigby SE, Barr AD, Clayton M, A review of Pochhammer-Chree dispersion in the Hopkinson bar, Proceedings of the Institution of Civil Engineers-Engineering and Computational Mechanics 171 (1) (2018) 3–13.
[43] Booker R. Velocity dispersion of isotropic rods of square cross section vibrating in the lowest-order longitudinal mode. J Acoust Society Am 1969;45 (5):1284–6.
[44] Spinner S, Reichard T, Tefft W. A comparison of experimental and theoretical relations between Young's modulus and the flexural and longitudinal resonance frequencies of uniform bars. J Res National Bureau Standards. Section A, Phys Chem 1960;64(2):147.
[45] Rossing TD, Russell DA. Laboratory observation of elastic waves in solids. Am J Phys 1990;58(12):1153–62.
[46] Chevalier Y, Vinh JT, Longitudinal vibration of rods: Material characterization and experimental dispersion curves, Mechanical Characterization of Materials and Wave Dispersion: Instrumentation and Experiment Interpretation (2013) 271–303.
[47] Brizard D. An impact test to determine the wave speed in SHPB: Measurement and uncertainty. J Dyna Behavior Mater 2020;6(1):45–52.
[48] Shin H. Pochhammer-Chree equation solver for dispersion correction of elastic waves in a (split) Hopkinson bar. Proc Inst Mech Eng, Part C: J Mech Eng Sci 2021. 0954406220980509.
[49] Shin H. Manual for calibrating sound speed and Poisson's ratio of (split) Hopkinson bar via dispersion correction using Excel and Matlab templates. Data 2022;7(5):55.
[50] GRAS 46BF-1 1/4 LEMO Free-field Standard Microphone Set, URL:https://www.grasacoustics.com/products/measurement-microphone-sets/traditional-power-supply-lemo/product/686-46bf-1, Last accessed on 2022-10-17.
[51] Engineer BA. The mechanical and resonant behaviour of a dry coupled thickness-shear PZT transducer used for guided wave testing in pipe line. Brunel University; 2013. Ph.D. thesis.
[52] Carta G. Correction to Bishop's approximate method for the propagation of longitudinal waves in bars of generic cross-section. European Journal of Mechanics-A/Solids 2012;36:156–62.
[53] Mindlin R, McNiven H. Axially symmetric waves in elastic rods. Columbia University. New York Department of Civil Engineering and Engineering Mechanics; 1958. Tech. rep..
[54] Anderson SP. Higher-order rod approximations for the propagation of longitudinal stress waves in elastic bars. J Sound Vib 2006;290(1–2):290–308.
[55] Gorham D. A numerical method for the correction of dispersion in pressure bar signals. J Phys E: Sci Instrum 1983;16(6):477.
[56] Bragov AM, Lomunov AK, Lamzin DA, Konstantinov AY. Dispersion correction in split-Hopkinson pressure bar: theoretical and experimental analysis. Continuum Mech Thermodyn 2019:1–13.
[57] Legg M, Bradley S, Experimental measurement of acoustic guided wave propagation in logs, in: 19th International Nondestructive Testing and Evaluation of Wood Symposium, Rio de Janeiro, Brazil, 2015, pp. 681–688.